© 2017. Published by The Company of Biologists Ltd | Journal of Experimental Biology (2017) 220, 4589-4599 doi:10.1242/jeb.154641

RESEARCH ARTICLE

Pharmacological analysis of the transmembrane action potential configuration in myoepithelial cells of the spontaneously beating heart of the ascidian *Styela rustica in vitro*

Vladimir A. Golovko[1,*], Igor A. Kosevich[2] and Mikhail A. Gonotkov[1]

ABSTRACT

The mechanisms of action potential (AP) generation in the myoepithelial cells of the tunicate heart are not yet well understood. Here, an attempt was made to elucidate these mechanisms by analyzing the effects of specific blockers of K^+, Na^+ and Ca^{2+} currents on the configuration of transmembrane APs and their frequency in the spontaneously beating ascidian heart. In addition, an immunocytochemical analysis of heart myoepithelial cells was performed. Staining with anti-FMRF-amide and anti-tubulin antibodies did not reveal any nerve elements within the heart tube. Treatment with 1 mmol l^{-1} TEA (I_K blocker) resulted in depolarization of heart cell sarcolemma by 10 mV, and inhibition of APs generation was recorded after 3 min of exposure. Prior to this moment, the frequency of AP generation in a burst decreased from 16–18 to 2 beats min^{-1} owing to prolongation of the diastole. After application of ivabradine (3 or 10 µmol l^{-1}), the spontaneous APs generation frequency decreased by 24%. Based on these results and published data, it is concluded that the key role in the automaticity of the ascidian heart is played by the outward K^+ currents, Na^+ currents, activated hyperpolarization current I_f and a current of unknown nature I_X.

KEY WORDS: Tunicate, Blockers, Ion channels

INTRODUCTION

The heart rhythm in mammals is initiated and regulated by a group of specialized cells located around the sinoatrial node artery (Li et al., 2014). These pacemaker cells are spontaneously activated by several inward (I_{CaT}, $I_{Ca,L}$ and I_f) and outward currents (I_K) sensitive to the sarcolemma potential, with a contribution from relatively potential-independent leakage current ($I_{b,Na}$), Na^+/K^+-ATPase current (I_{NaK}) and Na–Ca exchange current (I_{NaCa}). According to molecular genetic data, the Tunicata are a sister group to the vertebrates (Simoes-Costa et al., 2005; Salvador-Recatala et al., 2006), with the close evolutionary relationship between them being more evident during embryonic stages (Davidson, 2007). In particular, the human heart on days 25–40 of fetal development is structurally similar to the tunicate heart (Sizarov et al., 2011).

The tunicate heart is a tubular, valveless organ composed of a single layer of striated myoepithelial cells and enclosed in a stiff pericardial sac (von Skramlik, 1938; Waldrop and Miller, 2015). The blood is driven through the circulatory system by peristaltic contractions of the myocardium, which proceed in a spiral wringing motion and thereby prevent blood backflow (see Movie 1). Cardiac myocytes are interconnected by gap junctions, as in the mammalian heart (Weiss et al., 1976; Kriebel, 1967; Lorber and Rayns, 1977). The myocardial and pericardial tubes are fused to each other at the raphe that runs along the abdominal side of the heart.

The ascidian heart shows spontaneous electrical activity of myogenic type. Impulses and contractions periodically arise at one end of the heart tube and spread throughout its length (Anderson, 1968; Waldrop and Miller, 2015). A burst of action potentials (APs) is followed by a pause, and then the initiating impulse is generated at the opposite end. Thus, it appears that there are two clusters of spontaneously depolarizing cells at each end of the heart tube. However, this has not been consistently confirmed in studies on the ascidian heart automaticity, and the cellular mechanisms that initiate and regulate this process are not yet well understood (Hellbach et al., 2011).

In this study, a pharmacological approach has been used for the first time to evaluate the pattern of transmembrane APs in the spontaneously beating ascidian heart. In particular, we have analyzed the effects of specific blockers of K^+, Na^+ and Ca^{2+} currents on AP morphology and heart rate and also performed an immunocytochemical analysis of myoepithelial cells.

MATERIALS AND METHODS

Animals

Ascidians *Styela rustica* Linnaeus 1767 (Ascidiacea, Tunicata) (n=23; body mass 6±1 g, body height 65±5 mm) were collected by SCUBA divers from a depth of 2–10 m in the vicinity of the White Sea Biological Station, Moscow State University (Kandalaksha Bay, Karelia, Russia; 66°34′N, 33°08′E), in July–August 2013. Prior to experiments, the animals were kept in aquariums with running seawater at 8±1°C for 1–8 days, as described previously (Kuzmin et al., 2012).

All experiments were planned and carried out so as to minimize the number of animals used and their exposure to stress. The use of the tunicate in the laboratory does not raise any ethical issues, and therefore needs no approval from regional and local research ethics committees. The field sampling did not involve endangered or protected species, and, in accordance with local guidelines, no permission for collecting the material was required.

Isolated heart preparations

Part of the tunic was removed, the ascidian was placed with the buccal siphon on the right, and the visceral cavity was cut open on the basal side. The longitudinal muscle layer was then cut to expose the heart (a translucent tube enclosed in the pericardium, 4–6 mm long) located between the pharyngeal sac and the stomach. The

[1]Institute of Physiology, Komi Science Centre, Ural Branch, Russian Academy of Sciences, 50 Pervomayskaya St., Syktyvkar 167982, Russia. [2]Faculty of Biology, M.Lomonosov Moscow State University, Moscow 119991, Russia.

*Author for correspondence (golovko@physiol.komisc.ru)

V.A.G., 0000-0002-5150-9291

Received 26 December 2016; Accepted 28 September 2017

Journal of Experimental Biology (2017) 220, 4589-4599 doi:10.1242/jeb.154641

List of symbols and abbreviations

4-AP	4-aminopyridine
AP	action potential
APD_{20}	AP duration at 20% repolarization
APD_{50}	AP duration at 50% repolarization
APD_{90}	AP duration at 90% repolarization
APD_{100}	AP duration at 100% repolarization
ATP	adenosine triphosphate
BS	blocking solution
*Ciona*KChIP	potassium channel interacting protein
CionaK_v4	voltage-gated potassium channel
DD	diastolic depolarization
dV/dt_{max}	maximal upstroke velocity
EGTA	ethylene glycol tetraacetic acid
$I_{Ca,L}$	L-type Ca^{2+}-current
I_{CaT}	transient Ca^{2+}-current
I_f	hyperpolarization activated current
I_{KCa}	Ca^{2+}-dependent potassium current
I_{Kr}	rapid delayed rectifier K^+-current
I_{Ks}	slowly delayed rectifier K^+-current
I_{NaCa}	Na–Ca exchange current
I_{NaK}	sodium–potassium pump current
I_{to}	transient outward K^+-current
I_X	nifedipine-insensitive current
SR	sarcoplasmic reticulum
TEA	tetraethylammonium
V_3	velocity of final repolarization phase

heart tube was ligated at the nearest free end (usually at the dorsal side) and carefully detached throughout its length, taking care to avoid stretching. The isolated heart was placed in fresh seawater and, after a 30- to 40-min adaptation period, contractions were video-recorded under an Olympus stereo microscope type SZ51 (Fig. 1A).

Immunocytochemistry

Immunocytochemical analysis was performed with eight heart preparations: three hearts were analyzed immediately after their dissection from the ascidians, and five hearts after electrophysiological experiments. The pericardium was cut open, and the heart in the pericardium was placed in the experimental chamber, allowed to adapt in seawater, incubated in 5% $MgCl_2$ solution in fresh seawater for 15 min and fixed with 4% paraformaldehyde (Fluka, Germany) solution in 0.1 mol l^{-1} PBS for 15 min at room temperature.

For immunocytochemical staining, the fixed material was washed with permeabilization solution [0.3% Triton-X100 (Ferak, Berlin, Germany) and 0.1% Tween 20 in PBS] for 30 min, 0.4 mol l^{-1} glycine (Sigma-Aldrich, St Louis, MO, USA) for 40 min and 0.1% casein (Sigma-Aldrich) for 10 min; treated with three portions of blocking solution (BS) [3% BSA (Sigma-Aldrich), 0.3% Triton X100 and 0.1% Tween 20 in PBS] for 1 h each; and incubated with primary antibodies diluted in BS for 30 h at 4°C.

Primary antibodies were as follows: rabbit polyclonal anti-FMRF-amide (Chemicon, USA; 1:2000); mouse monoclonal anti-acetylated α-tubulin (Sigma-Aldrich, 1:1000); and mouse monoclonal anti-tyrosinated α-tubulin (Sigma-Aldrich, 1:1600). The last two antibodies were also used as a mixture.

Thereafter, the specimens were washed in four portions of BS (3 h each) and incubated with secondary antibodies for 10 h at 4°C. We used Alexa Fluor 546-conjugated donkey anti-rabbit IgG (Molecular Probes, Eugene, OR, USA; A10040), Alexa Fluor 488-conjugated donkey anti-mouse IgG (Molecular Probes, A21202), FITC-conjugated goat anti-mouse and TRITS-conjugated goat anti-rabbit antibodies (Pierce Biotechnology, Waltham, MA, USA), all diluted 1:500.

The specimens were then washed with BS for 2 h and stained with Alexa Fluor 647 phalloidin or rhodamine phalloidin (Molecular Probes, 1:100 in PBS) for 2 h at room temperature. After rinsing with three portions of permeabilization solution (10 min each), they were additionally stained with Hoechst 33342 nuclear stain (1 µg ml^{-1}; Molecular Probes, H21492) for 10 min, rinsed in PBS and mounted on a coverslip in 90% glycerol with 25 mg ml^{-1} 1,4-diazabicyclo(2,2,2)octane (DABCO; Aldrich-Chemie, Germany).

The preparations were examined under a Nikon A1 confocal microscope (Japan). Longitudinal optical sections were obtained at a step of 0.2–4 µm, depending on magnification. Z-projections were generated with ImageJ v. 1.50a software (National Institutes of Health, Bethesda, MD, USA) and processed in Adobe Photoshop CS5 Extended v. 12.0.3 x32 (Adobe Systems, San Jose, CA, USA).

Electrophysiological experiments

The pericardium was cut open, and the heart was placed in a bath with running filtered natural seawater bubbled with a mixture of 95% O_2 and 5% CO_2 at 15±1°C. The composition of the water was as follows: 280 mmol l^{-1} NaCl, 6 mmol l^{-1} KCl, 1.6 mmol l^{-1} $NaHCO_3$, 36 mmol l^{-1} $MgCl_2$, 7 mmol l^{-1} $CaCl_2$, 19 mmol l^{-1} Na_2SO_4, 0.5 mmol l^{-1} KBr and 0.5 mmol l^{-1} NaF. Water salinity in

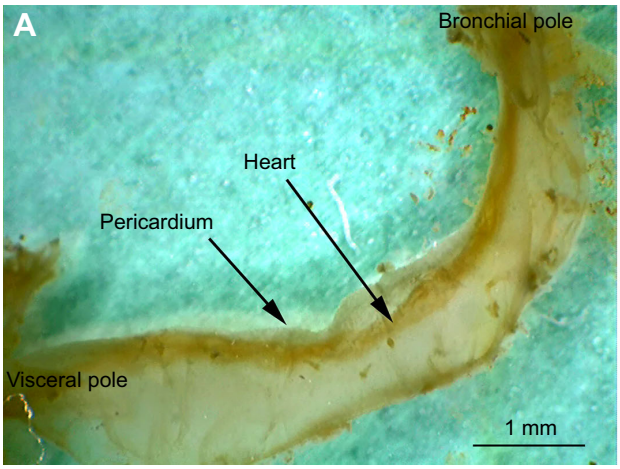

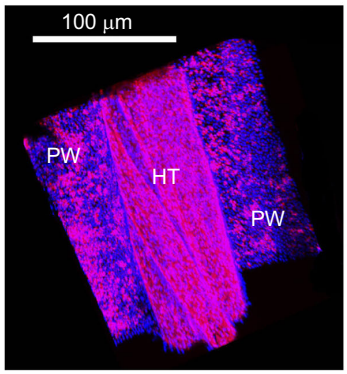

Fig. 1. The *Styela rustica* heart. (A) General view of the isolated *S. rustica* heart within the pericardium. (B) 3D reconstruction of the heart segment (framed in Fig. 3) after double staining with Hoechst 33342 (blue) and Rhodamine Phalloidin (red). PW, pericardium wall; HT, heart tube.

Journal of Experimental Biology

Journal of Experimental Biology (2017) 220, 4589-4599 doi:10.1242/jeb.154641

the White Sea is 24‰; its pH was adjusted to 8.1±0.2 (Kuzmin et al., 2012).

Only spontaneously beating isolated hearts with the pericardium were used in the experiment. The AP amplitude of myoepithelial heart cells in the control remained stable for 3–5 h. Transmembrane APs from the interior side of the heart were recorded with glass microelectrodes (40–50 MΩ) filled with 2.7 mol l^{-1} KCl and connected to a high-input impedance amplifier, digitized and analyzed using special software (L-card, Moscow, Russia; PowerGraph Professional v. 3.3 9, DISoft, Russia). The following AP parameters were documented and analyzed: AP amplitude (mV); overshoot (mV); resting potential (mV); cycle length (ms); AP duration at 20, 50, 90 and 100% repolarization (APD_{20}, APD_{50}, APD_{90} and APD_{100}, respectively); maximal upstroke velocity (dV/dt_{max}; V s^{-1}); velocity of final repolarization phase (V_3; V s^{-1}); and heart rate (beats min^{-1}).

Chemicals and drugs

Nifedipine (AppliChem, Darmstadt, Germany), 4-AP (AppliChem), EGTA (Sigma-Aldrich), lidocaine (Sigma-Aldrich) and TEA (AppliChem) were dissolved in bidistilled water; ivabradine (Servier, Suresnes, France) was dissolved in seawater. The drugs were added in the bath to the required concentration.

Statistical analysis

The data from each experiment (n_{cells}=4–8) are expressed as means±s.d. and were processed statistically by Student's *t*-test or Wilcoxon's test for paired samples using Microsoft Office Excel and PowerGraph Professional v.3.3.9. Differences were considered significant at $P<0.05$.

RESULTS

Features of heart morphology and cellular organization

The ascidian heart is tubular, valveless and enclosed in the pericardium. As shown by immunochemical staining, the pericardium consists of a single layer of cells that have no contractile filaments (Fig. 2A). The heart wall is also one cell-layer thick and consists of cross-striated myoepithelial contractile cells (Fig. 2C). These cells are diamond-shaped, approximately 4.0±0.5 µm in diameter and 12±2 µm long (n=14; Fig. 2B).

The heart wall (myocardium) is formed by an invagination of the pericardium, and there is a raphe along the line of connection between the myocardium and pericardium. The cells of the raphe have no contractile elements, but the cytoskeleton is prominent in these cells (Fig. 2A,C).

The contractile structures of the myoepithelial cells (represented by actin filaments) extend parallel to their long axes, which are oriented obliquely to the main heart axis. The contractile parts of the cells constitute the basal zone of the heart wall, which faces the cardiac lumen. Their apical parts contain one or two nuclei with distinct nucleoli and diffuse chromatin. Mononucleated and binucleated cells are of the same size, which may be evidence for proliferation of the myoepithelial cells (Fig. 2A). The well-developed tubulin cytoskeleton underlies the outer cell membrane (Fig. 2). In general,

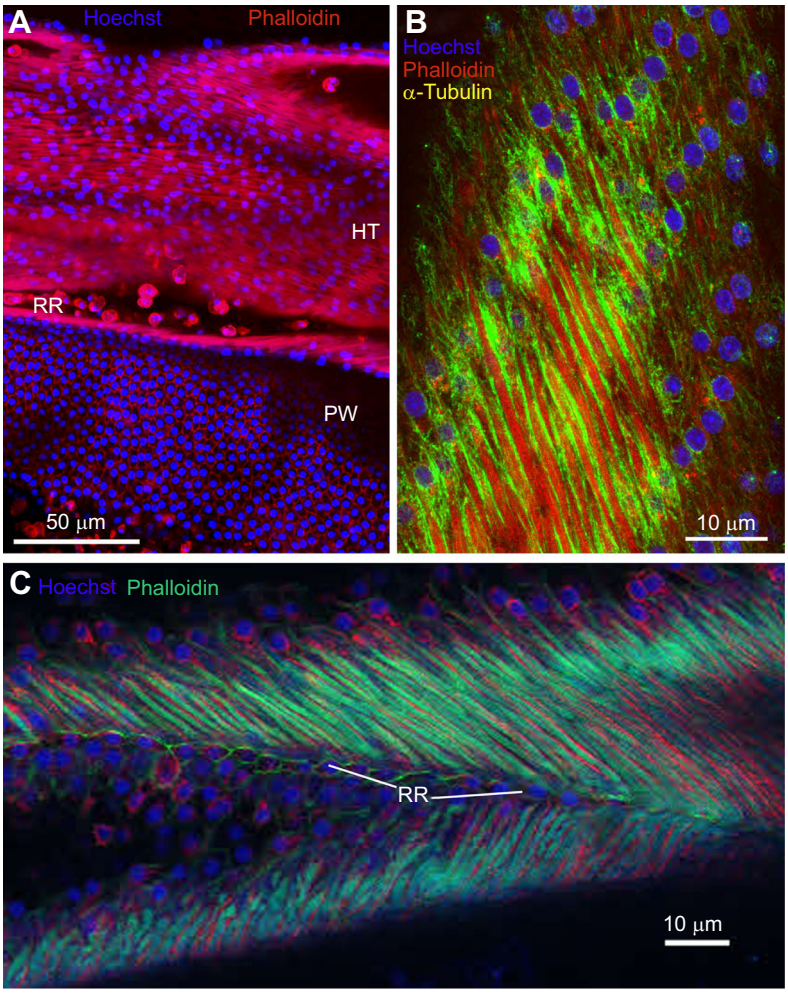

Fig. 2. Immunocytochemical analysis of the *S. rustica* heart and pericardium. (A) Z-projection of the heart as viewed from the pericardium cavity, staining for actin (Rhodamine Phalloidin, red). The nuclei (here and below) are stained with Hoechst 33342 (blue). Actin-positive staining is observed only in the heart tube (HT); cells of the single-layered pericardium wall (PW) and the raphe region (RR) contain no contractile elements. (B) Z-projection of the heart wall as viewed from the pericardium cavity, staining for actin (red) and α-tubulin (green). The wall remains slightly convex. Staining for α-tubulin shows that microtubules underlie the cell membrane and surround myofibrils and the nuclei. (C) Z-projection of heart tube wall as viewed from its lumen (the heart tube was cut longitudinally). Staining for actin with Alexa Fluor 647 phalloidin (green).

Journal of Experimental Biology (2017) 220, 4589-4599 doi:10.1242/jeb.154641

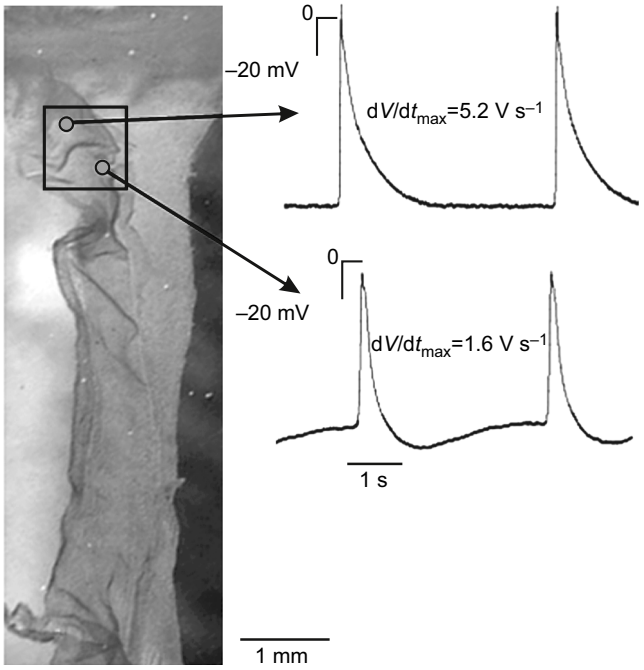

Fig. 3. A photo of *S. rustica* heart with intact pericardium and examples of two action potential (AP) types, without (upper) and with (lower) diastolic depolarization.

the cellular organization of the *S. rustica* heart revealed by the immunocytochemical method conforms to the data on heart ultrastructure in *Ascidia sidneyensis* (Kalk, 1970) and *Ascidia obliqua* (Martynova and Nylund, 1996), except for the presence of the distinct tubulin cytoskeleton and the absence of cilia in *S. rustica*.

The results of staining with anti-FMRF-amide and anti-α-tubulin antibodies were negative, suggesting the lack of nerve elements in the pericardium and the heart tube. This may be regarded as evidence that the nervous system has no direct effect on the rhythmic activity of the heart, although the presence of other neuropeptides cannot be excluded.

General characterization of heart electrical activity

With respect to characteristics of APs, two types of myoepithelial cells were distinguished: cells generating APs with slow diastolic depolarization (DD; pacemaker cells) or without it (contractile, or working cells) (Fig. 3).

The latter generated APs with higher amplitude (92±6 mV), duration (APD_{100}=2.5±0.3 s) and maximum upstroke velocity (dV/dt_{max}=7±1 V s^{-1}) (n_{hearts}=13) compared with the pacemaker cells (amplitude 71±6 mV, dV/dt_{max}=1.6±0.3 V s^{-1}; n_{hearts}=5; Table 1). In all isolated ascidian hearts, APs at 15°C were recorded in cycles, with bursts consisting of 11 to 30 spikes (19 ±6 impulses; frequency per burst 16±2 beats min^{-1}, without taking into account pauses). Such an episode was followed by a pause of 9 to 35 s (25±6 s, n_{hearts}=11), and then a burst of APs was generated at the opposite end of the heart tube (Fig. 4A).

The myoepithelial cells of the ascidian heart are thin and contain smaller amounts of contractile proteins and mitochondria than cardiomyocytes of the animals that are more advanced in evolution. Therefore, the role of mitochondria is less important, and glycolysis appears to be the main source of energy in the ascidian heart. It should be noted that the last cycle of AP generation before the pause preceding the switch of dominance between the pacemaker centers is, on average, 30% longer than in the burst. As a result, the direction of blood flow is reversed, which is important for the functioning of the open circulatory system of the Tunicata.

To evaluate the electrophysiological interaction between the two automaticity centers, the spontaneously contracting heart tube was cut into two equal parts, one containing the hypobranchial pacemaker and the other the visceral pacemaker. After the heart tube was cut into two segments, the direction of electrical impulse conduction in either segment remained unchanged, and AP generation continued with pauses. Each part generated APs for 40–60 s, which was followed by a pause of 20–60 s. Then AP generation was resumed, with the direction of excitation spread remaining unchanged. The parts with the hypobranchial and visceral pacemakers generated APs with a frequency of 18±2 beats min^{-1} (n_{hearts}=6) and 16±1 beats min^{-1} (n_{hearts}=3), respectively (Fig. 5A). This frequency did not differ significantly from that in the whole isolated heart (Fig. 5B,C), and the same was true of other AP parameters.

Table 1. Summary of the effects of blockers on action potential (AP) parameters in *Styela rustica* heart cells

Parameter	Resting potential (mV)	Overshoot (mV)	APD_{20} (ms)	APD_{50} (ms)	APD_{90} (ms)	APD_{100} (ms)	Cycle length (s)	dV/dt_{max} (V s^{-1})	V_3 (V s^{-1})
Control (n=13)	–90±4 (–83 to –95)	5±4 (3–12)	90±13 (60–120)	290±30 (220–330)	900±110 (700–1200)	2500±300 (1800–3200)	3.5±0.5 (14–16 beats min^{-1})	5±1 (4–7)	1.5±0.5 (1–2)
Control (n=6)	–92±6	6±3	110±15	420±30	1100±120	2750±250	3.6±0.7	4.7±0.3	0.15±0.02
Ivabradine, 3 µmol l^{-1} (n=6)	–89±4	6±3	105±10	320±25	980±100	3000±1250	4.5±0.6*	4.4±0.4	0.16±0.03
Control (n=5)	–90±5	6±2	80±15	260±25	900±120	2000±300	3.9±0.3	4.9±0.3	1,4±0,5
Lidocaine, 1 mmol l^{-1} (n=5)	–93±6	1±1	120±20*	330±40*	1150±100*	2400±300	3.5±0.4	3.7±0.4*	0.8±0.3*
Control (n=4)	–88±3	6±1	120±20	250±20	950±80	2450±320	5±1	5.2±0.2	2±0,3
4-AP, 5 mmol l^{-1} (n=4)	–90±4	10±2*	190±30*	220±10	910±30	2200±310	4.8±0.7	6±1	1.7±0.3
Control (n=4)	–86±4	5+4	80±10	250±40	800±90	1980±200	5±2	5.2±0.8	1,7±0.8
TEA, 1 mM (n=4)	–80±3	4±1	90±7*	280±30	840±50	1970±220	20±4*	3.9±0.2	1.1±0.2

ADP_{20}, APD_{50}, APD_{90}, APD_{100}, action potential duration at 20, 50, 90 and 100% repolarization; dV/dt_{max}, maximal upstroke velocity; V_3, velocity of final repolarization phase; 4-AP, 4-aminopyridine; TEA, tetraethylammonium.
*Significantly different from control (0.01<P<0.05).

Journal of Experimental Biology (2017) 220, 4589-4599 doi:10.1242/jeb.154641

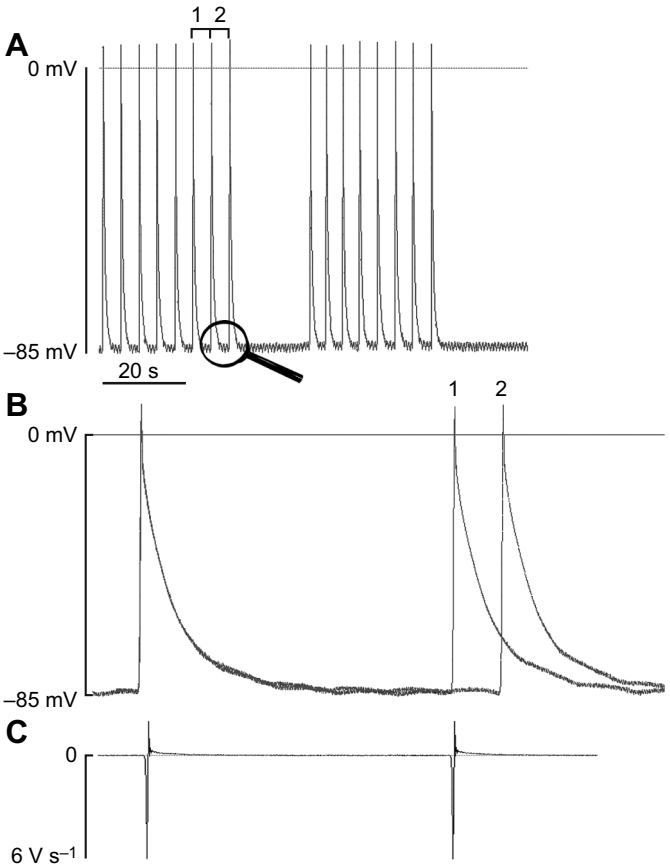

Fig. 4. Transmembrane APs of *S. rustica* heart myoepithelial cells. (A) A burst of APs is followed by a pause (in the center), after which the blood is pumped in the reverse direction. (B) Superposition of the second to last and last AP cycles before the pause shown on an expanded time scale (see area indicated by magnifying glass symbol in A). (C) Maximal upstroke velocity of APs (dV/dt_{max}).

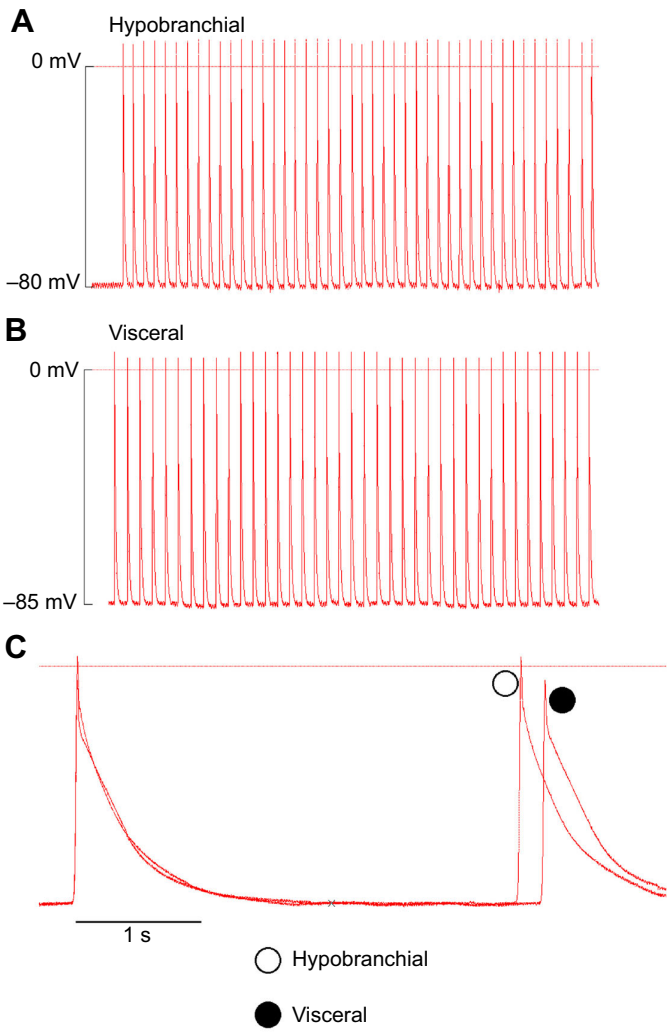

Fig. 5. Typical recordings of electrical activity. APs generated in the (A) hypobranchial and (B) visceral parts of the *S. rustica* heart (without pauses); (C) the same APs shown on an expanded time scale.

Effects of 4-AP as an I_K blocker

We evaluated the contribution of K^+ currents to the morphology of AP repolarization phase, which lasts for approximately 2 s and is therefore comparable to the diastole phase (1.7 s long). Under the effect of 2.5 mmol l^{-1} 4-AP, a blocker of ultrarapid K^+ current (I_{Kur}) and transient outward K^+ current (I_{to}), the sarcolemmal APs of myoepithelial heart cells without slow DD increased from 89 to 99 mV because of an increase in overshoot (Fig. 6Ai,ii). APD_{20} increased by a factor of 1.5 compared with the control (Fig. 6Aiii).

It should be noted that a rise in plateau level and reduction of APD_{50} were recorded in cells without slow DD. The maximum rate of AP increase at phase 0 was 30% higher, and the rate of final repolarization was two to three times higher compared with the control (Fig. 6Aiii). Against this background, however, a cessation of AP generation in cells without slow DD was recorded at minute 7±1 of 4-AP exposure (Fig. 6Aii).

After the hearts were washed and the main AP parameters were restored, the concentration of 4-AP was increased from 2.5 to 5 mmol l^{-1}. In this variant, the above effects on APs morphology were more distinct, and the inhibition of AP generation was recorded at minute 3±1 of exposure (Fig. 6Aii,iii).

These results suggest that the effect of 4-AP is dose-dependent and reversible. The currents sensitive to 4-AP, supposedly I_{to} and I_K, play a key role in generating AP repolarization and automaticity in the ascidian heart cells.

Effects of TEA as an I_K blocker

Treatment with 1 mmol l^{-1} TEA resulted in depolarization of heart cell sarcolemma by 10 mV (from –93 to –83 mV) and reduction of AP amplitude owing to decrease in overshoot. APD_{20} was also prolonged by 10–13% compared with the control (Fig. 6Bi,ii), with APD_{50} and APD_{100} remaining unchanged. Pairwise comparisons (control–effect) revealed a decrease in dV/dt_{max} (on average, from 5.1±1.1 to 3.9±1 V s^{-1}) and an almost 1.5-fold reduction in the rate of final repolarization in all the hearts used in the experiment (Fig. 6Cii). The inhibition of AP generation was recorded at minute 3±1. Prior to this moment, the frequency of AP generation in a burst decreased from 20 to 2 beats min^{-1} because of prolongation of the diastole (Fig. 6Bii,Cii).

Effects of ivabradine as an I_f blocker

After application of ivabradine (3 or 10 µmol l^{-1}), the spontaneous AP generation frequency decreased by an average of 24±3% (n_{hearts}=4) compared with the control (Fig. 7).

The deceleration of the heart rhythm in all preparations was due to prolongation of the diastole (Fig. 7C). The number of APs per burst decreased fourfold, and the duration of pauses between the bursts was reduced by a factor of 1.5, from 28 to 20 s (Fig. 7A,B). These results suggest the existence of an ivabradine-sensitive current that retards the

Journal of Experimental Biology (2017) 220, 4589-4599 doi:10.1242/jeb.154641

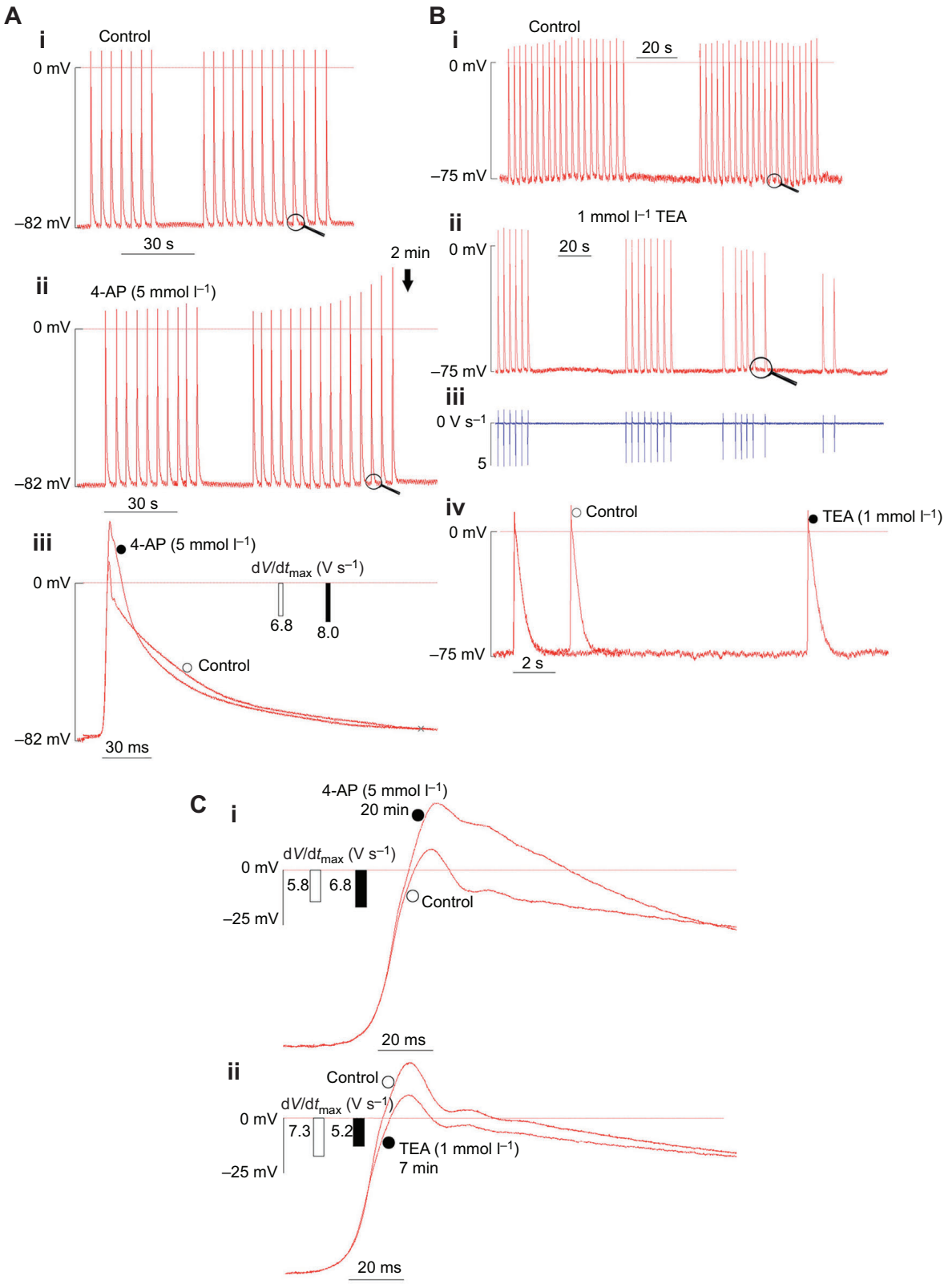

Fig. 6. Effects of 4-AP and TEA on the spontaneously beating *S. rustica* heart. (A) Effect of 4-AP: (Ai) control; (Aii) treatment with 4-AP resulted in higher AP amplitude because of an increase in overshoot, but AP generation against this background ceased within a short time; (Aiii) superposition of APs recorded in the control and under the effect of 4-AP (see areas indicated by magnifiying glass symbols in Ai and Aii, respectively). (B) Effects of TEA: (Bi) control; (Bii, Biv) treatment with TEA resulted in reduction of AP amplitude and frequency of spontaneous AP generation and (Biii) decrease in dV/dt_{max}, with subsequent block of heart electrical activity. (Biv) Comparison of two APs on an expanded time scale (see areas indicated by magnifying glass symbols in Bi and Bii). (C) Comparison of the effects of (Ci) 4-AP and (Cii) TEA on an expanded time scale.

Journal of Experimental Biology

Journal of Experimental Biology (2017) 220, 4589-4599 doi:10.1242/jeb.154641

generation of diastolic depolarization of pacemaker cells in the ascidian heart by an average of 25%. This current (supposedly I_f) affects the frequency of AP generation, and its inhibition results in more frequent alternation of dominance between the two pacemaker centers.

Effects of lidocaine as an I_{Na} blocker

Lidocaine (1 mmol l^{-1}) reduced the amplitude of APs by an average of 6 mV on account of decrease in overshoot. After 2–5 min of exposure, the peak of AP at 20% repolarization level (APD_{20}) was lengthened from 75 to 120 ms (+60%) in all heart preparations (n=6), with dV/dt_{max} in cells without slow DD decreasing from 4.9±0.3 to 3.7±0.4 V s^{-1} (–24%, P<0.05; Fig. 8A, Table 1).

Upon further exposure, the total period of AP generation increased by an average of 14%. The number of APs per burst remained unchanged, but the pause became 1.5–2.0 times longer (Fig. 8Aii). It should be noted that AP generation in 50% of heart preparations was blocked after 10±2 min. The effect of lidocaine was reversible. These results suggest that the lidocaine-sensitive current (supposedly I_{Na}) plays a more important role in the automaticity of ascidian heart cells compared with the L-type Ca^{2+} current.

Effects of nifedipine as an $I_{Ca,L}$ blocker

To elucidate the role of inward L-type Ca^{2+} current ($I_{Ca,L}$) in AP morphology, nifedipine (1–10 µmol l^{-1}), a specific blocker of L-type voltage-operated Ca^{2+} channels, was added to the perfusing solution.

Unexpectedly, no signs of change (relative to the control) were observed in the morphology of APs in cells without slow DD, including the frequency of their generation (n_{hearts}=5; Fig. 8Bi–iii, Table 1). Therefore, we consider that the role of $I_{Ca,L}$ in the morphology of APs generated by the pacemaker cells of the ascidian heart is less important than that of I_{Na}.

Effects of EGTA as a Ca^{2+} chelator

To estimate the contribution of free cytosolic Ca^{2+} and the Ca^{2+} content in the sarcoplasmic reticulum (SR), a high-affinity Ca^{2+} chelator (2 mmol l^{-1} EGTA) was added to the bath solution (Fig. 9).

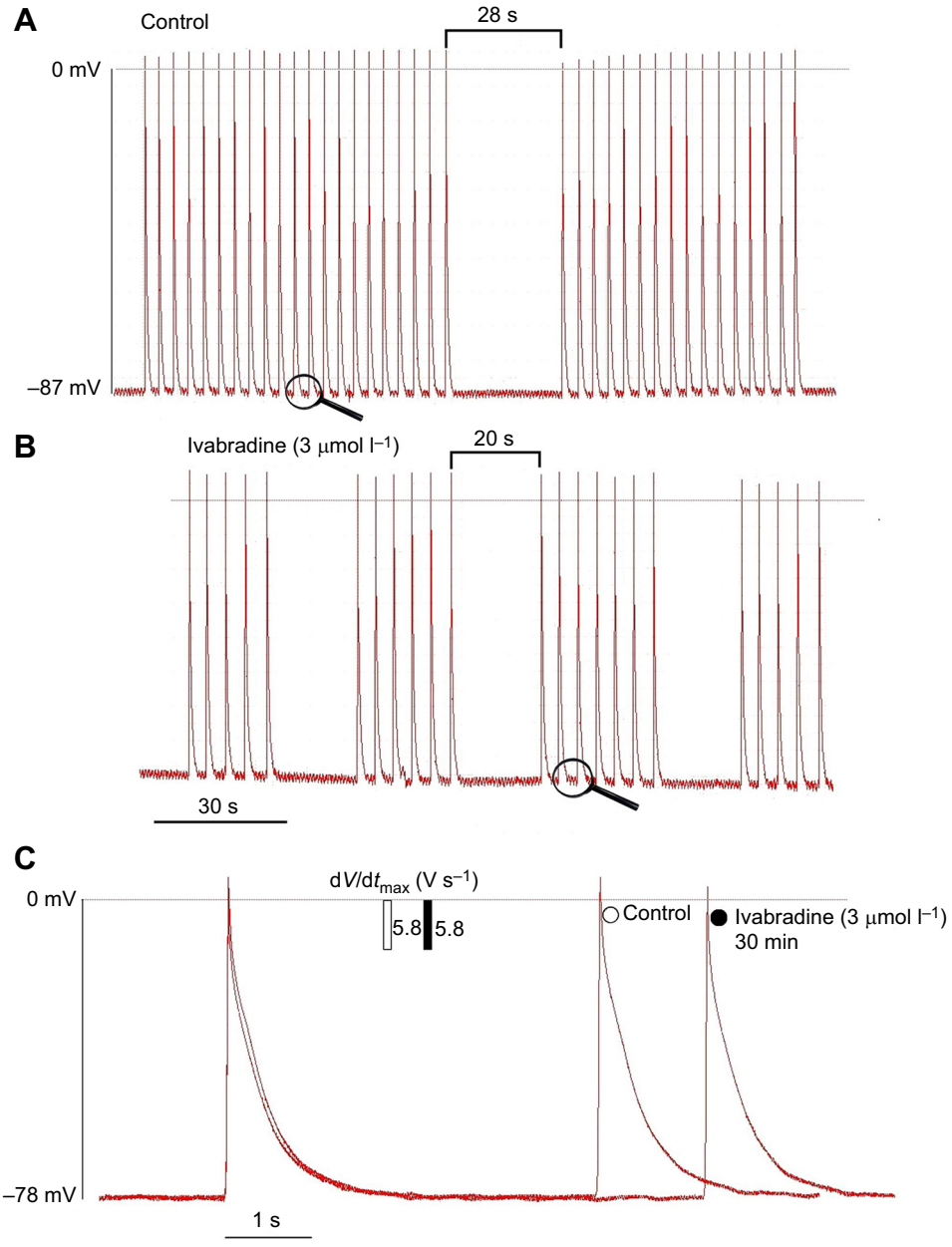

Fig. 7. Effect of ivabradine on the spontaneously beating *S. rustica* heart. (A) Control. (B) Treatment with ivabradine. (C) Superposition of APs in A and B (see areas indicated by magnifying glass symbols) on an expanded time scale.

Journal of Experimental Biology (2017) 220, 4589-4599 doi:10.1242/jeb.154641

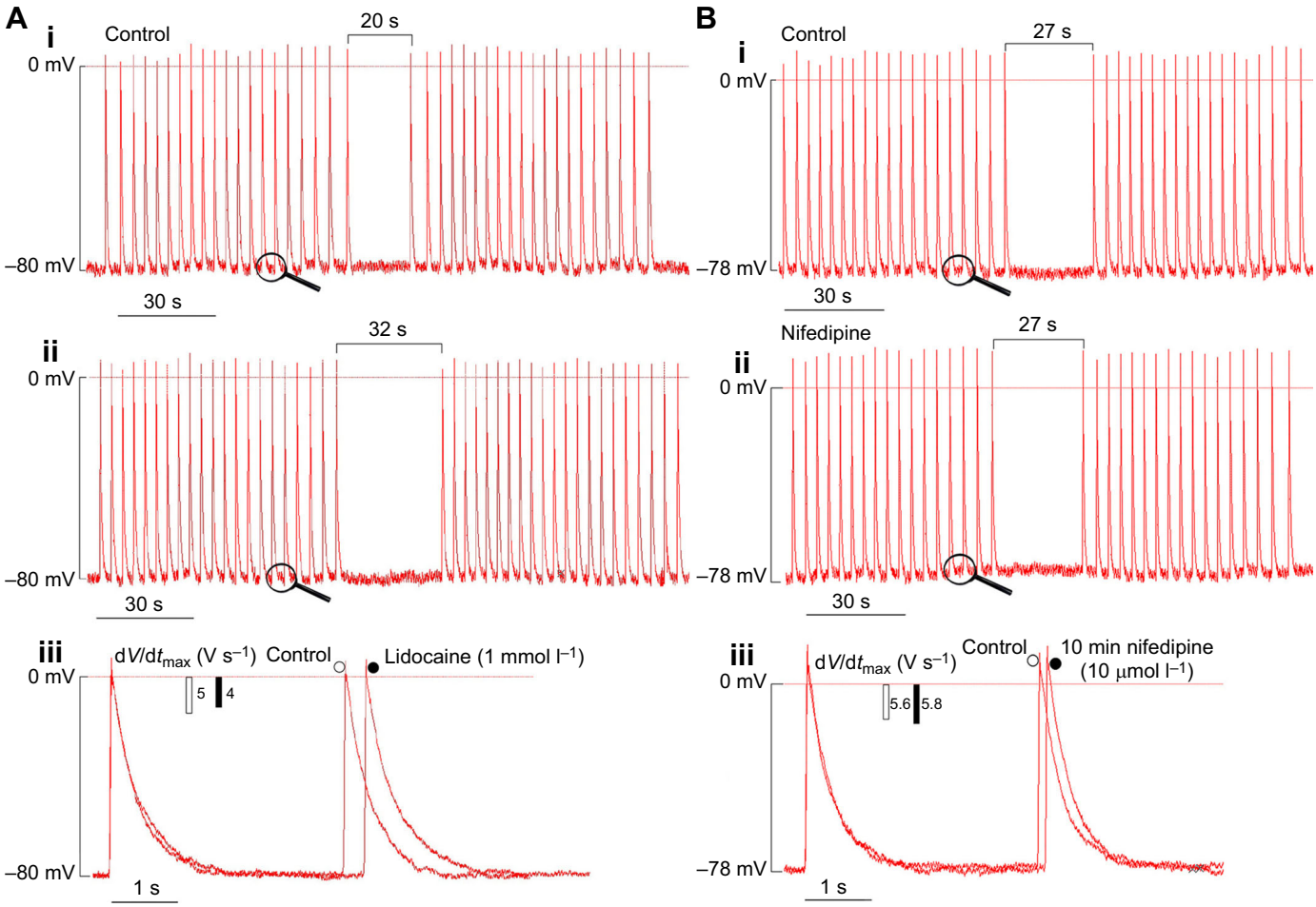

Fig. 8. Effects of lidocaine and nifedipine on the morphology of APs. (A) Effect of lidocaine. (Ai) Typical recorded APs in the control; (Aii) lidocaine exposure; (Aiii) superposition of APs recorded in the control and with lidocaine (see areas indicated by magnifying glass symbols in Ai and Aii, respectively). (B) Effect of nifedipine. (Bi) Microelectrode recorded APs in control; (Bii) application of nifedipine; (Biii) superposition of the APs recorded in the control and nifedipine treatments on an expanded time scale (see areas indicated by magnifying glass symbols in Bi and Bii, respectively).

After 5-min exposure, the amplitude of APs became lower, which was due to a decrease in overshoot (Fig 9A,B). After 30-min exposure, APD_{50} lengthened by a factor of 1.4 (from 180 to 260 ms) and APD_{90} by a factor of 1.5 (from 0.90 to 1.4 s); dV/dt_{max} and the velocity of final repolarization became 10% and 60% lower than in the control, respectively. It should be noted that reduction in the duration of diastole was greater than prolongation of AP peak; as a result, the frequency of AP generation increased by an average of 15% relative to the control (Fig. 9C). These changes were often accompanied by arrhythmia of different types, with bigeminal rhythms being most frequent.

DISCUSSION

Morphofunctional characteristics

The ascidian heart is a valveless tube composed of a single myoepithelial cell layer. Myogenic impulses periodically arise at one end of the tube and spread throughout its length. A burst of contractions evoked by electrical impulses is followed by a pause of 25±6 s, and then the initiating impulse is generated at the opposite end. We have shown for the first time that the pause in the functioning of the pacemaker center is preceded by prolongation of the AP generation cycle by an average of 30%, compared with this period during the burst. It is logical to assume that this decrease in the frequency of AP generation is explained by a temporary decrease in the I_f density. Cutting the heart tube into two equal segments has no effect on the number of APs per burst and the duration of the pause, with the direction of electrical impulse conduction remaining unchanged in either segment. Therefore, the initiating impulses in the intact heart are generated by pacemakers located at both ends (the hypobranchial and visceral pacemakers). It appears that the pause after an AP burst occurs because the cells of the dominant pacemaker are depleted of the ATP necessary for active transport. Potassium currents (I_{to} and I_K) definitely play an important role in shaping the morphology of APs in the ascidian heart cells. There is experimental evidence that the electrogenic sodium–potassium pump current (I_{NaK}) is generated in pacemaker cells (Irisawa et al., 1993; Sakai et al., 1996), with AMP being necessary for this process.

Identification of I_{to} and I_K and their impact on AP generation

According to our data, APs generated by ascidian cardiac myoepithelial cells without slow DD are triangular in shape (Figs 3 and 4B, Table 1). In this respect, they are similar to APs of vertebrate atrial myocardial cells. Recent studies on the genome of the tunicate *Ciona interstinalis* have identified and cloned the genes encoding a K_v4 potassium channel (*Ciona*K_v4) and a KChIP subunit modulating its activity (*Ciona*KChIP), and revealed their phylogenetic relationship with the ancestral forms common to mouse, human and rat (e.g. Salvador-Recatala et al., 2006). We have supposed that

Journal of Experimental Biology (2017) 220, 4589-4599 doi:10.1242/jeb.154641

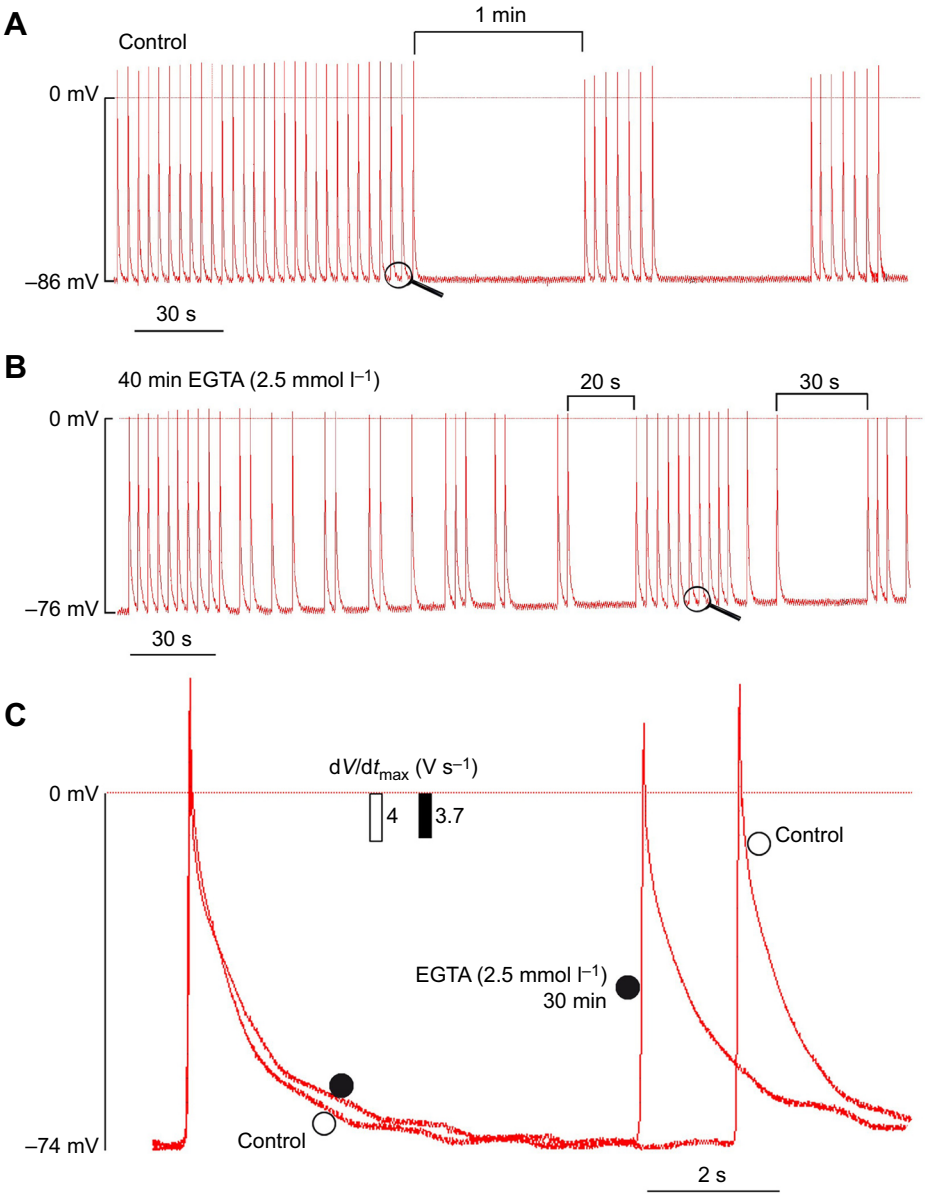

Fig. 9. Effect of EGTA on the spontaneously beating *S. rustica* heart. (A) Control. (B) Treatment with EGTA. (C) EGTA markedly reduced the spontaneous AP firing rate compared with the control.

the *Ciona*K_v4 channels mainly conduct the transient outward K^+ current I_{to}, which is sensitive to 4-AP (Cordeiro et al., 2013; Gonotkov and Golovko, 2013). This current is usually activated at V_m from –20 up to –50 mV, but it may be recorded as the sum of I_{to} and I_K, because it is difficult to discriminate between these currents by electrophysiological methods. It has been shown that I_K is activated 10 times as slowly as I_{to}, having an activation threshold of –30 mV (Bouchard and Fedida, 1995); it is insensitive to 4-AP but is blocked by a millimolar concentration of TEA; conversely, I_{to} is blocked by 4-AP but is insensitive to TEA (Himmel et al., 1999). Therefore, we have used selective pharmacological blockers of these currents, namely, 4-AP, which blocks I_{to} (Apkon and Nerbonne, 1991; Barry and Nerbonne, 1996), and TEA, which attenuates I_K (Dixon et al., 1996; Nerbonne and Kass, 2005). The inhibition of either I_{to} or I_K has proved to result in the suppression of spontaneous electrical activity. The increase in the AP plateau level recorded in the experiment on heart perfusion with the seawater containing 4-AP (Fig. 6Aiii) may be explained by a stronger blocking of I_{to} than I_{Kur}. The occurrence of the plateau phase at more positive values of the membrane potential results in activation of delayed-rectifier K^+ current, which accelerates the final repolarization phase (Sanchez et al., 2014). The dV/dt_{max} and maximal diastolic potential (E_{max}) values in myoepithelial cells of the ascidian myocardium are approximately 7 V s^{-1} and –80 mV, respectively. A study on human embryonic stem cell-derived cardiomyocytes with slow DD and similar AP parameters has shown that a Ca^{2+}-dependent potassium current (I_{KCa}) is generated in these cells (Weisbrod et al., 2013). It may well be that the same is true of the pacemaker cells of the ascidian heart (Fig. 10A).

Role of I_f

Experiments on the role of ivabradine-sensitive current I_f in the rate of AP generation in the ascidian heart showed that ivabradine (an antagonist of HCN channels) increased the AP cycle length by an average of 25% (Fig. 7, Table 1) but did not block automaticity. The rhythm slowed down because of increase in the duration of the diastole, which was accompanied by reduction in the number of APs per burst and in the intervals between bursts by factors of 4 and 1.5, respectively, compared with the control (Fig. 10B). The contribution of I_f to the total AP cycle length in the ascidian heart is similar to that in the rabbit heart (Yaniv et al., 2012) and mouse

Journal of Experimental Biology (2017) 220, 4589-4599 doi:10.1242/jeb.154641

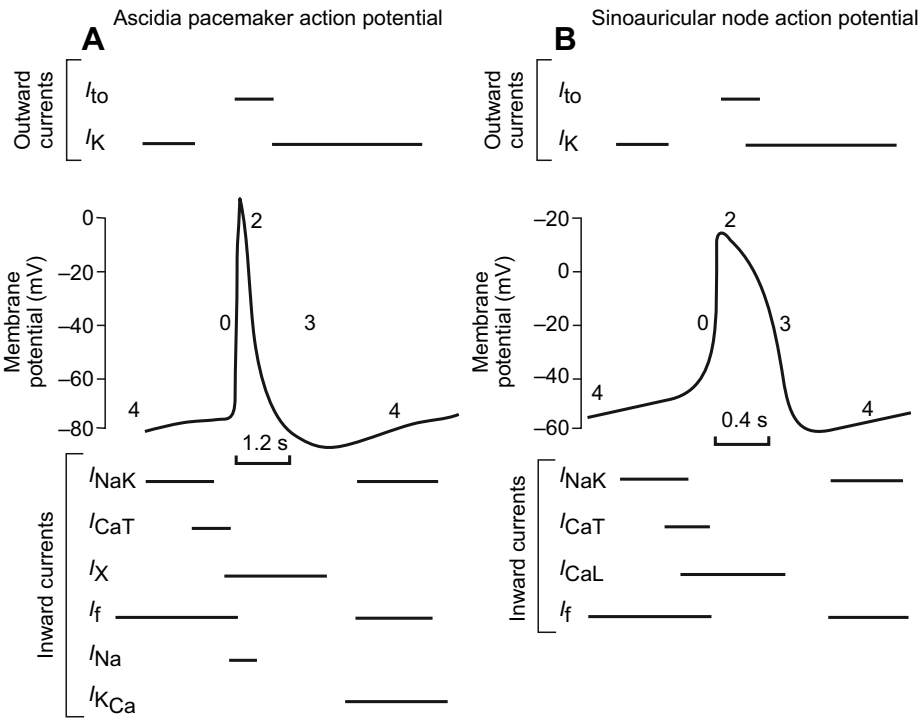

Fig. 10. Hypothetical scheme describing the mechanisms of pacemaker AP generation in tunicate and vertebrate hearts. (A) Tunicate; (B) vertebrate. The numbers near the curves indicate the AP phases: (0) upstroke, (2) plateau, (3) final repolarization and (4) slow DD. Horizontal bars indicate the periods when the channels are active. Scheme A is compiled from our data on the effects of selective blockers of I_f, I_{Na}, I_K and I_X on the ascidian heart (data on I_{KCa} are from Weisbrod et al. 2013). Scheme B is compiled from data by Zaza et al. (2009), Gonotkov and Golovko (2013) and Golovko and Gonotkov (2014).

heart (Golovko and Gonotkov, 2014). There are grounds to consider that the I_f current flows through the HCN channels hyperpolarized by cyclic nucleotides. Thus, there is evidence for homonomy between three isoforms of HCN channels of the tunicate *Ciona interstinalis* (Ci-HCN1–Ci-HCN3) and the NCN channels of vertebrates (Okamura et al., 2005; Jackson et al., 2007).

EGTA does not completely block the heart's electrical activity

To study the effects of Ca^{2+} buffering on the intracellular Ca^{2+} dynamics, we used EGTA as a high-affinity, slow-binding Ca^{2+} chelator that is known to reduce primarily the content of free diastolic Ca^{2+} in the cytosol (Bers and Guo, 2005). Compared with fast-binding chelators such as BAPTA, EGTA allows Ca^{2+} to diffuse to greater distances after its release to the cytosol through the RyR_2 receptor (Terentyev et al., 2002; Kornyeyev et al., 2010). Addition of EGTA to the bath solution which binds to Ca^{2+} released from the SR resulted in a consequent increase in AP generation frequency and disturbances of the heart rhythm against the background of prolongation of the final repolarization phase and reduction in the duration of diastole. It is known that EGTA disturbs or blocks the functioning of the 'calcium clock' in mammals (Kornyeyev et al., 2010). These effects in ascidians may be even stronger because of poorly developed SR and a low rate of Ca^{2+} uptake, which excludes the probability of a pacemaker function of the SR in the ascidian heart cells. The decrease in $[Ca^{2+}]_i$ under the effect of EGTA accelerates restitution of Ca^{2+} release from mitochondria and reduces the influx of Ca^{2+} through the sarcoplasmic membrane (Cheng et al., 1996; Kornyeyev et al., 2010). This is why Ca^{2+} is a strong arrhythmogenic factor, and increase in its intracellular concentration results in higher frequency of AP generation. However, the effects of EGTA in the ascidian proved to be much weaker than in vertebrates. Thus, vertebrate myocardial cells incubated with 2 mmol l^{-1} EGTA showed triggered activity with a sharp drop in AP amplitude after 10–12 min (with these effects being irreversible), whereas the pacemaker activity in the ascidian heart was retained for more than 60 min at a higher concentration of the chelator.

Thus, the results of inhibitor analysis performed in this study show that the lidocaine-sensitive current I_{Na} and the nifedipine-insensitive current I_X of unknown nature are involved in the generation of the rapid depolarization phase in the myoepithelial cells of the ascidian heart (Fig. 10A). After repolarization is completed, the K^+ currents are attenuated, while the ivabradine-sensitive current I_f and transient current I_{CaT} current are activated. The Na^+/K^+-ATPase current I_{NaK} is generated throughout this phase. It appears that I_{CaT} channels allow the uptake of a small amount of Ca^{2+} that is sufficient for activation of K^+ current (I_{KCa}). In our opinion, the main difference in the mechanism of AP generation between the ascidian heart cells and the cells of the mammalian sinoatrial node is that the key role in the automaticity of the ascidian heart is played by K^+ currents sensitive to 4-AP and TEA.

Acknowledgements

The authors are grateful to Prof. Aleksandr B. Tzetlin, director of the White Sea Biological Station, for general support of this study and to Prof. D. Abramochkin, Dr V. Kuzmin and Dr G. Sukhova, who kindly provided the equipment for the experiments.

Competing interests

The authors declare no competing or financial interests.

Author contributions

Conceptualization: V.A.G.; Methodology: V.A.G., I.A.K., M.A.G.; Validation: M.A.G.; Formal analysis: I.A.K., M.A.G.; Investigation: V.A.G., I.A.K., M.A.G.; Resources: I.A.K.; Data curation: V.A.G., M.A.G.; Writing - original draft: V.A.G.; Writing - review & editing: V.A.G.; Visualization: I.A.K., M.A.G.; Project administration: V.A.G.; Funding acquisition: V.A.G.

Funding

This research was funded by the Ural Branch, Russian Academy of Sciences (grant 15-5-4-11).

Supplementary information

Supplementary information available online at http://jeb.biologists.org/lookup/doi/10.1242/jeb.154641.supplemental

References

Anderson, M. (1968). Electrophysiological studies on initiation and reversal of the heart beat in *Ciona interstinalis*. *J. Exp. Biol.* **49**, 363-385.

Apkon, M. and Nerbonne, J. M. (1991). Characterisation of two distinct depolarization-activated K^+ currents in isolated adult rat ventricular myocytes. *J. Gen. Physiol.* **97**, 973-1011.

Barry, D. M. and Nerbonne, J. M. (1996). Myocardial potassium channels: electrophysiological and molecular diversity. *Annu. Rev. Physiol.* **58**, 363-394.

Bers, D. M. and Guo, T. (2005). Ca^{2+} signaling in cardiac ventricular myocytes. *Ann. N.Y. Acad. Sci.* **1047**, 86-98.

Bouchard, R. and Fedida, D. (1995). Closed- and open-state binding of 4-aminopyridine to the cloned human potassium channel Kv1.5. *J. Pharmacol. Exp. Ther.* **275**, 864-876.

Cheng, H., Lederer, M. R., Lederer, W. J. and Cannell, M. B. (1996). Calcium sparks and (Ca^{2+})I waves in cardiac myocytes. *Am. J. Physiol.* **39**, C148-C159.

Cordeiro, J. M., Nesterenko, V. V., Sicouri, S., Goodrow, R. J., Jr, Treat, J. A., Desai, M., Wu, Y., Doss, M. X., Antzelevitch, C. and Di Diego, J. M. (2013). Identification and characterization of a transient outward K^+ current in human induced pluripotent stem cell-derived cardiomyocytes. *J. Mol. Cell. Cardiol.* **60**, 30-46.

Davidson, B. (2007). *Ciona interstinalis* as a model for cardiac development. *Semin. Cell Dev. Biol.* **18**, 16-26.

Dixon, J. E., McDonald, H., Cohen, I. S. and McKinnon, D. (1996). Role of the Kv4.3 K^+ channel in ventricular muscle. A molecular correlate for the transient outward current. *Circ. Res.* **79**, 659-668.

Golovko, V. A. and Gonotkov, M. A. (2014). The contributions of currents involving potassium ions in the formation of action potentials in true pacemaker cells of mouse sinoauricular node. *Cardiovasc. Res.* **103**, 102.

Gonotkov, M. A. and Golovko, V. A. (2013). 4-aminopyridine lengthened the plateau phase of action potentials in mouse sinoauricular node cells. *Bull. Exp. Biol. Med.* **59**, 4-6.

Hellbach, A., Tiozzo, S., Ohn, J., Liebling, M. and de Tomaso, A. W. (2011). Characterization of HCN and cardiac function in a colonial ascidian. *J. Exp. Zool.* **313A**, 1-11.

Himmel, H. M., Wettwer, E., Li,Q. and Ravens, U. (1999). Four different components contribute to outward current in rat ventricular myocytes. *Am. J. Physiol.* **277**, H107-H118.

Irisawa, H., Brown, H. F. and Giles, W. (1993). Cardiac pacemaking in sinoatrial node. *Physiol. Rev.* **73**, 197-227.

Jackson, H. A., Marshall, C. R. and Accilli, E. A. (2007). Evolution and structural diversification of hypopolarization-activated cyclic nucleotide-gated channel genes. *Physiol. Genomics* **29**, 231-245.

Kalk, M. (1970). Organization of a tunicate heart. *Tissue Cell Res.* **2**, 99-118.

Kornyeyev, D., Reyes, M. and Escolar, A. L. (2010). Luminal Ca^{2+} content regulates intracellular Ca^{2+} release in subepicardial myocytes of intact beating mouse hearts: effect of exogenous buffers. *Am. J. Physiol. Heart Circ. Physiol.* **298**, H2138-H2153.

Kriebel, M. (1967). Conduction velocity and intracellular action potentials of the tunicate heart. *J. Gen. Physiol.* **50**, 2097-2107.

Kuzmin, V. S., Volkova, E. V. and Sukhova, G. S. (2012). Cholinergic regulation of body wall muscle contraction of the ascidia *Styela rustica* (Linnaeus, 1767). *Russ. J. Mar. Biol.* **38**, 228-236.

Lorber, V. and Rayns, D. G. (1977). Fine structure of the gap junctions in the tunicate heart. *Cell Tissue Res.* **179**, 169-175.

Li, N., Csepe, T. A., Hansen, B. J., Dobrzinski, H., Higgins, R. S., Kilic, A., Mohler, P. J., Janssen, P. M., Biesiadeck, B. J. and Fedorov, V. V. (2015). Molecular mapping of sinoatrial node HCN channel expression in the human heart. *Circ. Arrhythm. Electrophysiol.* **8**, 1219-1227.

Martynova, M. G. and Nylund, A. (1996). DNA-synthesizing cells in the heart of *Ascidia obliqua* (Tunicata). *Biol. Bull.* **190**, 410-417.

Nerbonne, J. M. and Kass, R. S. (2005). Molecular physiology of cardiac repolarization. *Physiol. Rev.* **85**, 1205-1253.

Okamura, Y., Nishino, A., Murata, Y., Nakajo, K., Iwasaki, H., Ohtsuka, Y., Tanaka-Kunishima, M., Takahashi, N., Hara, Y., Yoshida, T. et al. (2005). Comprehensive analysis of the ascidian genome reveals novel insights into the molecular evolution of ion channel genes. *Physiol. Genomics* **22**, 262-282.

Sakai, R., Hagiwara, N., Matsuda, N., Kassanuki, H. Hosoda, S. (1996). Sodium–potassium pump current in rabbit sino-atrial node cells. *J. Physiol.* **490**, 51-62.

Salvador-Recatala, V., Gallin, W. J., Abbruzzese, J., Ruben, P. C. and Spencer, A. N. (2006). A potassium channel (Kv4) cloned from the heart of the tunicate *Ciona interstinalis* and its modulation by a KChIP subunit. *J. Exp. Biol.* **209**, 731-747.

Sánchez, C., Bueno-Orovio, A., Wettwer, E., Loose, S., Simon, J., Ravens, U., Pueyo, E, and Rodriguez, B. (2014). Inter-subject variability in human atrial action potential in sinus rhythm versus chronic atrial fibrillation. *PLOS ONE*. **9**, e105897.

Simoes-Costa, M., Vasconcelos, M., Sampaio, A., Cravo, R. M., Davidson, B. and Xavier-Neto, J. (2005). The evolutionary origin of cardiac chambers. *Dev. Biol.* **277**, 1-15.

Sizarov, A., Ya, J., de Boer, B. A., Lamers, W. H., Christoffels, V. M. and Moorman, A. F. (2011). Formation of the building plan of the human heart: morphogenesis growth and differentiation. *Circulation*. **213**, 1125-1135.

Terentyev, D., Viatchenko-Karpinski, S., Voldivia, H. H., Escolar, A. L. and Gyorke, S. (2002). Luminal Ca^{2+} controls termination and refractory behavior of Ca^{2+}-induced Ca^{2+} release in cardiac myocytes. *Circ. Res.* **91**, 414-420.

von Skramlik, E. (1938). Über den Kreislauf bei den niedersten Chordaten. *Ergebn. Biol.* **15**, 166-308.

Waldrop, L. D. and Miller, L. A. (2015). The role of the pericardium in the valveless, tubular heart of the tunicate *Ciona savignyi*. *J. Exp. Biol.* **218**, 2753-2763.

Weisbrod, D., Peretz, A., Ziskind, A., Binah, O. and Attali, B. (2013). SK4 $Ca2^+$-activated K^+ channel is a critical player in cardiac pacemaker derived from human embryonic stem cells. *Proc. Natl. Acad. Sci. USA* **110**, E1685-E1694.

Weiss, J., Goldman, Y. and Morad, M. (1976). Electromechanical properties of the single cell-layered heart of the tunicate *Boltenia ovifera*. *J. Gen. Physiol.* **68**, 503-518.

Yaniv, Y., Maltsev, V. A., Ziman, B. D., Spurgeon, H. A. and Lakkatta, E. G. (2012). The “funny” current (I(f)) inhibition by ivabradine at membrane potentials encompassing spontaneous depolarization in pacemaker cells. *Molecules.* **17**, 8241-8254.

Zaza, A., Wilders, R. and Opthof, T. (2009). Cellular Electrophysiology. In *Comprehensive Electrocardiology*, 2nd edn (ed. P. W. Macfarlane , A. van Oosterom, M.J. Janse J. Camm P. Kligfield and O. Pahlm), pp. 25-48. London: Springer.

Movie 1